QUANTUM PHASES OF DIPOLAR BOSONS IN BILAYER GEOMETRY

BY ARGHAVAN SAFAVI-NAINI, SEBNEM G. SÖYLER, GUIDO PUPILLO, HOSSEIN R. SADEGHPOUR, AND BARBARA CAPOGROSSO-SANSONE

SUMMARY

We present the zero temperature phase diagram of a system of ultra-cold bosons in a bilayer optical lattice as well as the finite temperature behavior of these phases using Quantum Monte Carlo (QMC) simulations by the Worm Algorithm (WA) [1].

Models describing strongly correlated lattice quantum systems have been the focus of intense theoretical studies in the past decade. The Fermi-Hubbard hamiltonian, potentially being the minimal model explaining high Tc superconductivity [2], and the Bose-Hubbard hamiltonian exhibiting the superfluid (SF)-Mott-insulator (MI) phase transition [3], are two paradigmatic examples. These models, although simple, are highly non-trivial as they reveal the important many-body physics of strongly correlated systems. Moreover, they can be experimentally realized using atomic and molecular quantum gases trapped in optical lattices [4,5].

More recently, due to experimental progress in trapping ground state polar molecules with strong electric dipole moments [7], and atoms with large permanent magnetic moments [6], quantum models with tunable, long-range and anisotropic interactions are within reach. Hence theoretical understanding of such systems is timely and compelling.

In the following letter we study a system consisting of dipolar particles confined in a pair of two-dimensional (2D) optical lattice layers, and with dipole moments polarized perpendicular to the planes. As a result of the anisotropic and long-range nature of the dipolar interaction between the particles, exotic quantum phases such as the pair-supersolid (PSS) and pair-superfluid (PSF) [among others] can be stabilized and survive up to temperatures of the order of nK. The schematic of this setup is shown in the top right panel of Figure 1(b). The 2D confinement is achieved by using a strong transverse trapping field, *e.g.* a 1D optical lattice with harmonic oscillator frequency $\omega_\perp$ and lattice spacing d_z. A large enough confinement provides the collisional stability of the setup [8] and creates a large potential barrier between the two layers which suppresses tunneling, thus preventing inter-layer hopping. The particles are further confined in plane by a 2D optical lattice with harmonic frequency ω and lattice spacing a. When $\hbar\omega > d^2/a^3$, k_BT (where d is the induced dipole moment and T the temperature), tunneling to an already occupied site is strongly suppressed [9], and particles can be treated in the hard-core limit.

The system is described by the extended Bose-Hubbard model:

$$H = -J \sum_{\langle i,j\rangle,\alpha} a_{i\alpha} a_{j\alpha} - \frac{1}{2} \sum_{i\alpha;j\beta} V_{i\alpha;j\beta} n_{i,\alpha} n_{j,\beta} - \sum_{i,\alpha} \mu n_{i,\alpha} \quad (1)$$

where i, j refer to the lattice sites, α, β refer to the layers and $a_{i,\alpha}$ and $a^\dagger_{i,\alpha}$ are the bosonic creation and annihilation operators respectively, with $(a^\dagger_{i,\alpha})^2 = 0$, $n_{i,\alpha} = a^\dagger_{i,\alpha} a_{i,\alpha}$. $\langle\ \rangle$ denotes summation over nearest neighbors only. The first term in the Hamiltonian describes the kinetic energy with in-plane hopping rate J. The second term is the dipole-dipole interaction given by

$$V_{i,\alpha;j\beta} = C_{dd}/4\pi[(1 - 3\cos 2\theta)/|r_{i,\alpha} - r_{j,\beta}|^3]$$

where $C_{dd} = d^2/\varepsilon_0(\mu_0 d^2)$ for electric (magnetic) dipoles. Lastly μ is the chemical potential which sets N, the number of particles present in the system.

In this setup the in-plane dipolar interaction, V_{dd}, is repulsive and isotropic while the interlayer interaction is anisotropic. We denote the repulsive nearest neighbor intralayer interaction by $V_{dd} = C_{dd}/4\pi a^3$ and the attractive interlayer dipole-dipole interaction between dipoles sitting on top of each other by $V_{dd}^\perp = 2C_{dd}/4\pi d_z^3$. We can tune the relative strength $V_{dd}/V_{dd}^\perp$ over a wide range of values by changing d_z. In what follows we consider same type and number of particles on each layer, and choose $d_z = 0.36a$ so that $V_{dd}^\perp/J < 10$ at half filling factor [10]. This choice allows us to access a parameter regime where particles on the same lattice site but on different layers can pair up to form a composite object. For

A. Safavi-Naini <safavin@mit.edu>, Massachusetts Institute of Technology, Cambridge, MA USA and ITAMP, Harvard-Smithsonian Centre for Astrophysics, Cambridge, MA 02138,
S.G. Söyler, The Abdus Salam International Centre for Theoretical Physics, Trieste, Italy;
G. Pupillo, Université de Strasbourg;
H.R. Sadeghpour, Harvard-Smithsonian Centre for Astrophysics, Cambridge, USA;
B. Capogrosso-Sansone, University of Oklahoma, Norman, OK, USA

a gas of RbCs molecules with d ≈1.25 D the above conditions will be satisfied for a < 500nm and dz < 200 nm at J < 120hHz.

We present results based on path integral Quantum Monte Carlo simulations by a two-worm algorithm [11] which allows for efficient sampling of paired phases. We have performed simulations of $L \times L = N_{sites}$ square lattices with L = 8,12,16, 20 and 24. We have set the dipole-dipole interaction cutoff to the third nearest neighbor. We found that, while using a larger cutoff did not change the simulation results (within error bars), super-solid phases (see below) cannot be stabilized at lower cutoff values.

The zero temperature phase diagram of model (1) is shown in Figure 1(a). The latter is symmetric about n = 0.5 due to the particle-hole symmetry (a consequence of the hard-core constraint). The observed phases are sketched in Figure 1(b).

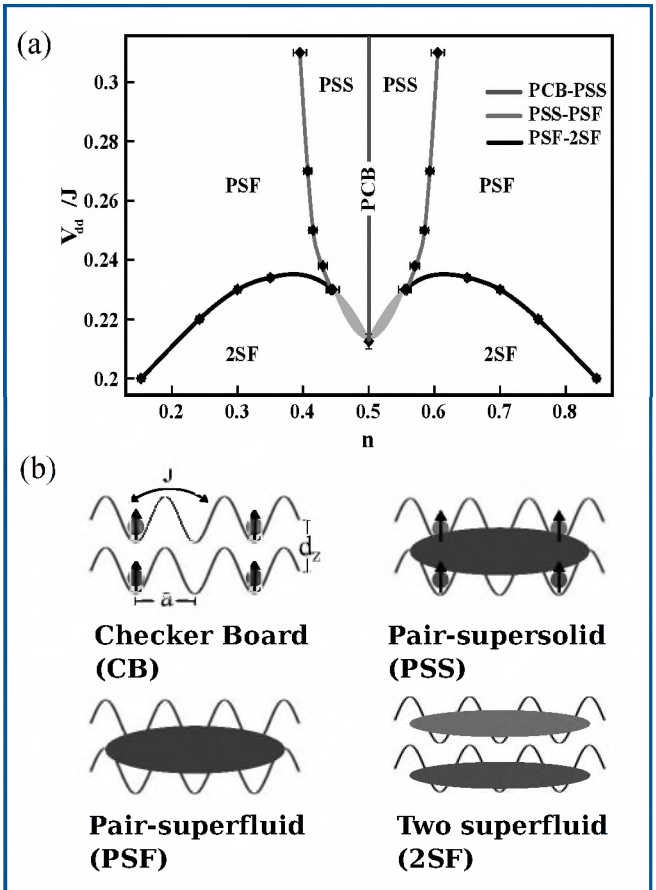

Fig. 1 (a) The zero temperature phase diagram of (1) as a function of the in-plane dipole-dipole interaction V_{dd}/J and the filling factor n. The diamonds show the QMC simulation results. In cases where the error bars are not visible, the error is within the symbol size. We were not able to resolve the phase boundaries in the shaded region. (b) A schematic representation of the phases. Each cloud represents an independent superfluid in the 2SF phase while the cloud in the PSS and PSF phases is a superfluid of the pairs.

At half-filling, $n = N/N_{sites} = 0.5$, when the in-plane repulsion is strong enough, *i.e.* $V_{dd}/J \geq 0.21 \pm 0.05$, a checkerboard (CB) solid of pairs (with every other site in each layer occupied) is stabilized. At this filling factor, the most energetically favorable configuration is a perfect CB crystal. The CB solid order is characterized by zero superfluidity and finite structure factor for each layer:

$$S(k)=\frac{1}{N}\sum_{r,r'}\exp\left[ik(r-r')\right]\langle n_r n_{r'}\rangle \qquad (2)$$

at reciprocal lattice vector $\mathbf{k} = (\pi,\pi)$. In this phase $\psi_{i\alpha} = \psi_{i\beta} = \Psi = 0$ where $\psi_{i\alpha} = \langle a_{i\alpha}\rangle$ is the single-particle order parameter and $\Psi = \langle a_{i\alpha}\, a_{i\beta}\rangle$ is the pair order parameter. In the paired CB phase atoms across the layers are strongly paired due to attractive interlayer interactions. Hence the particles sit on top of each other and the system can be envisioned as a solid of pairs [12,13].

Upon doping the CB solid with particles or holes we enter the PSS phase. The latter displays both, broken translational symmetry, $S(\pi,\pi) \neq 0$, *i.e.* diagonal long range order, and non-vanishing pair order parameter Ψ, *i.e.* off-diagonal long range order, while $\psi_{i\alpha} = \psi_{i\beta} = 0$. Figure 2(a) shows $S(\pi,\pi)$ (left y-axis) and the superfluid stiffness of pairs ρ_{PSS} (right y-axis) as a function of n, at $V_{dd}/J = 0.238$ for different system sizes. Both quantities are non-zero for a finite range of densities

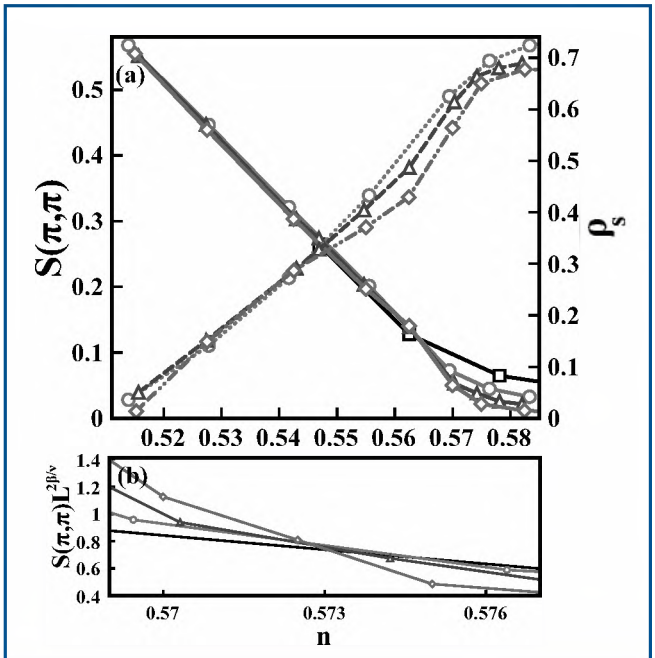

Fig. 2 (a) The structure factor $S(\pi,\pi)$ (solid lines, left y-axis) and superfluid density ρs (dashed lines, right y-axis) for the PSS-PSF transition at $V_{dd} = 0.238J$ for L = 8,12,16,20 and 24 and at T/J = 1/(1.5L). The arrow indicates the phase boundary. (b) The scaled structure factor $S(\pi,\pi)L^{2\beta/\nu}$ vs. n using the critical exponents of the Ising universality class in (2+1) dimensions, $2\beta/\nu = 1.0366$.

implying a stable PSS phase. The off-diagonal order present in the PSS phase is a result of extra particle or hole pairs (quasi-particles) which delocalize on top of the CB solid. Upon further doping, the system can no longer sustain the solid order and PSS disappears in favor of PSF via an Ising transition in (2+1)-dimensions. In the PSF phase only the off-diagonal long range order of PSS survives. The critical point (indicated by an arrow in Fig. 2(a)) is determined using finite size scaling with scaling coefficients $2\beta/\nu = 1.0366$ [14]. Figure 2(b) shows the scaled quantity $S(\pi,\pi)L^{1.0366}$ as a function of n. The crossing of the curves corresponds to the quantum critical point where the finite size effects disappear.

Finally, the system forms two independent superfluids (2SF) as V_{dd}/J is lowered at constant n. In this phase $\psi_{i\alpha} = \psi_{i\beta} \neq 0$ and the pair order parameter is trivially non-zero, $\Psi \neq 0$. Unlike the zero density limit, where a bound state is always formed [15], at finite density, many body effects favor 2SF, resulting in a finite threshold for stabilization of pairing.

We have also studied the finite temperature behavior of the system and determined critical temperatures at which the above described quantum phases disappear. The SF-normal transition is of Kosterlitz-Thouless (KT) type [16]. We determine its critical temperature $T_{KT} = \pi\hbar^2\rho_s(T_{KT})/2$ by finite size scaling as described in [17].

Figure 3 shows a plot of ρ_s vs. T/J at $V_{dd}/J = 0.20$ and n = 0.3 (corresponding to 2SF) for different system sizes. The finite size scaling procedure used to determine the critical temperature is shown in the inset. We find $T_{KT,2SF} \approx 0.255 \pm 0.005J$. For the PSF phase we find $T_{KT,PSF} \approx 0.08 \pm 0.01J$ at n = 0.3 and $V_{dd}/J = 0.25$. The lower critical temperature is due to a larger effective mass of the pairs which results in a lower effective hopping, a suppression of particle delocalization and consequently lower ρ_s.

The disappearance of the PSS phase proceeds in two successive stages. At n=0.38, $V_{dd}/J = 0.25$ and $T_{KT,PSS} \approx 0.060 \pm 0.005J$, first the superfluidity of excess particle (hole) pairs disappear leaving a normal liquid phase on top of the CB solid, reminiscent of a liquid crystal with $\rho_s = 0$ and $S(\pi,\pi) \neq 0$. Upon further increasing the temperature $S(\pi,\pi)$ becomes zero at $T_c \approx 0.3J$ through an Ising-type transition ($2\beta/\nu = 1/4$ in 2D). We estimate $T_{KT,PSS} <$ nK for a typical experimental setup with RbCs.

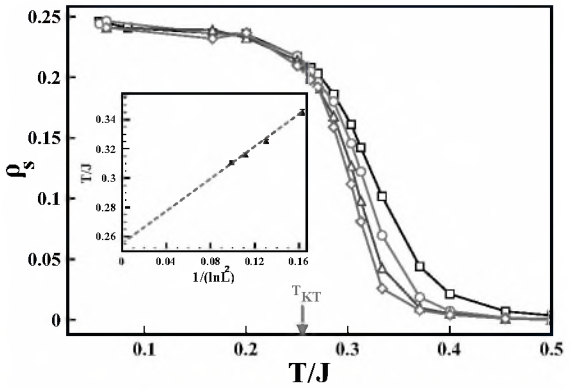

Fig. 3 Superfluid stiffness, ρs, as a function of temperature, T/J, at V_{dd}=0.20J and n=0.30 in the 2SF phase at L = 12,16,20 and 24. As temperature is increased the 2SF phase undergoes BKT phase transition at critical temperature T_{KT}. The error bars are within symbol size. The inset shows $T_{KT}(L)$ vs. $1/(\ln L)^2$. The dashed line is the linear fit to the simulation results (points). The y-intersect is the T_{KT} for an infinite size system.

In conclusion we have studied the quantum phases of dipolar bosons in a bilayer lattice geometry described by model (1) in the regime where pairing can be stabilized. We have observed a rich ground state phase diagram featuring pair-superfluidity, pair-supersolidity, independent superfluids and checkerboard solid phases. These phases are experimentally observable at temperatures of the order of nK.

REFERENCES

1. A. Safavi-Naini, S.G. Söyler, G. Pupillo, H.R. Sadeghpour and B. Capogrosso-Sansone, *arXiv*: 1208.5807.
2. P. A. Lee, N. Nagaosa, and X.-G. Wen, *Rev. Mod. Phys*. **78**, 17 (2006), and references therein.
3. M. P. A. Fisher, P. B. Weichman, G. Grinstein, and D.S. Fisher, P*hys. Rev.* **B 40**, 546 (1989).
4. D. Jaksch, C. Bruder, J.I. Cirac, C.W. Gardiner, and P. Zoller, *Phys. Rev. Lett.* **81**, 3108 (1998).
5. I. Bloch, J. Dalibard, and W. Zwerger, *Rev. Mod. Phys*. **80**, 885 (2008).
6. M. Lu, N. Q. Burdick, S.-H. Youn, and B. L. Lev, *Phys. Rev. Lett.* **107**, 190401 (2011).
7. K.-K. Ni *et al*., Science 322, 231 (2008); S. Ospelkaus *et al*., *Nat. Phys*. **4**, 622 (2008).
8. H. P. Büchler *et al*., Phys. Rev. Lett. 98, 060404 (2007); A. Micheli *et al*., *Phys. Rev.* **A 76**, 043604 (2007).
9. H. P. Büchler, A. Micheli, and P. Zoller, *Nat. Phys*. **3,** 726 (2007).
10. B. Paredes *et al*., *Nature* **429**, 277 (2004).
11. S.G. Söyler, B. Capogrosso-Sansone, N.V. Prokofev, B.V. Svistunov, *N. J. Phys*. **11**, 073036 (2009).
12. C. Trefzger, C. Menotti and M. Lewenstein, *Phys. Rev. Lett.* **103**, 035304 (2009).
13. B. Capogrosso-Sansone, *Phys. Rev.* **A 83** 053611 (2011).
14. M. Hasenbusch, K. Pinn, and S. Vinti, *Phys. Rev.* **B 59**, 11471 (1999).
15. J.R.Armstrong, *et al*., *EPL* **91**, 16001 (2010); M. Klawunn, *et al*., *Phys. Rev.* **A 82**, 044701 (2010).
16. J. M. Kosterlitz and D. J. Thouless, *J. Phys*. **C. 6**, 1973 (1181).
17. D. M. Ceperley and E. L. Pollock, *Phys. Rev.* **B 39**, 2084 (1989).